1 Purity monitor measurements

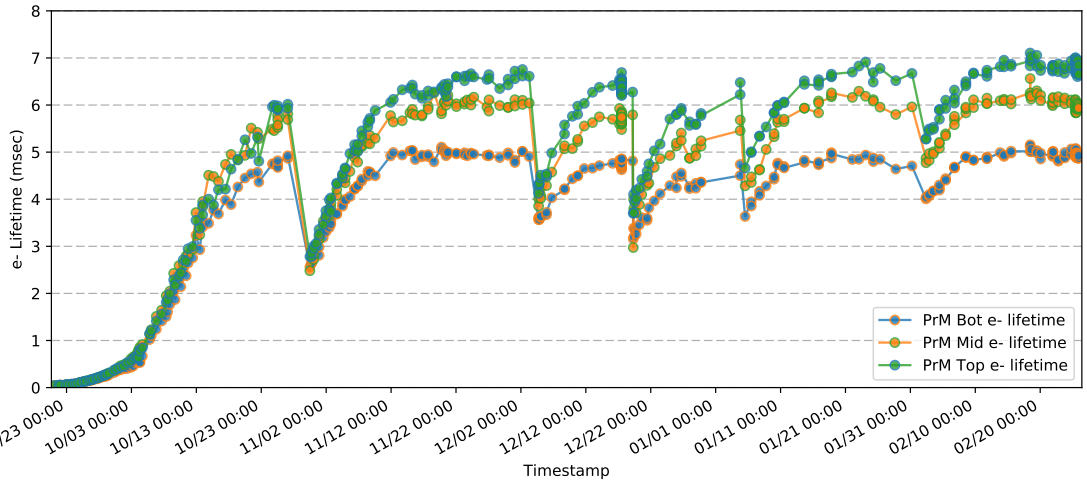

Figure 1: Electron lifetime as of Feb 2019 measured by the three purity monitors at three heights. Author: Jianming Bian, Ilsoo Seong, Casandra Morris, Andrew Renshaw, Stephen Pordes

Figure 1 shows electron lifetime as of Feb 2019 measured by the three purity monitors at three heights. The heights from the floor of the cryostats to the bottom (Bot), middle (Mid), and top (Top) purity monitors are 1.8 m, 3.7 m, and 5.6 m, respectively. By reporting sudden drops of electron lifetime (the dips in the figure), purity monitors have alerted the experiment solely to serious problems several times. The first time was for filter saturation during LAr filling, and the rest were re-circulation pump stoppages, false alarms, and problems from the cryostat-level gauges. These alerts are crucial to the ProtoDUNE-SP project's success, as they prevented situations which otherwise would have continued unnoticed for some time, with severe consequences to the ability to take any data. Neither the gas analyzers nor the TPC caught these problems in time.

A purity monitor is a miniature TPC. It is a double-gridded ion chamber which measures the lifetime of photoelectrons generated by a UV-illuminated gold photocathode to monitor the purity of LAr. The UV is generated by a xenon flash lamp and is delivered by optic fibers. The electron (e-) lifetime in LAr is inversely proportional to the electronegative impurity concentration. The fraction of electrons generated at the PrM cathode that arrive at the anode (Q_A/Q_C) after the drift time t is a measure of the e-lifetime τ: $Q_A/Q_C = e^{-t/\tau}$.

To optimize the precision and sensitivity of the lifetime measurement, the operation high voltages on purity monitor cathodes and anodes are tuned to make electron drift time 2.2 ms in the purity monitor.Q_A/Q_C is about 0.7 when electron lifetime reaches 6 ms.

2 Signal-to-noise ratio

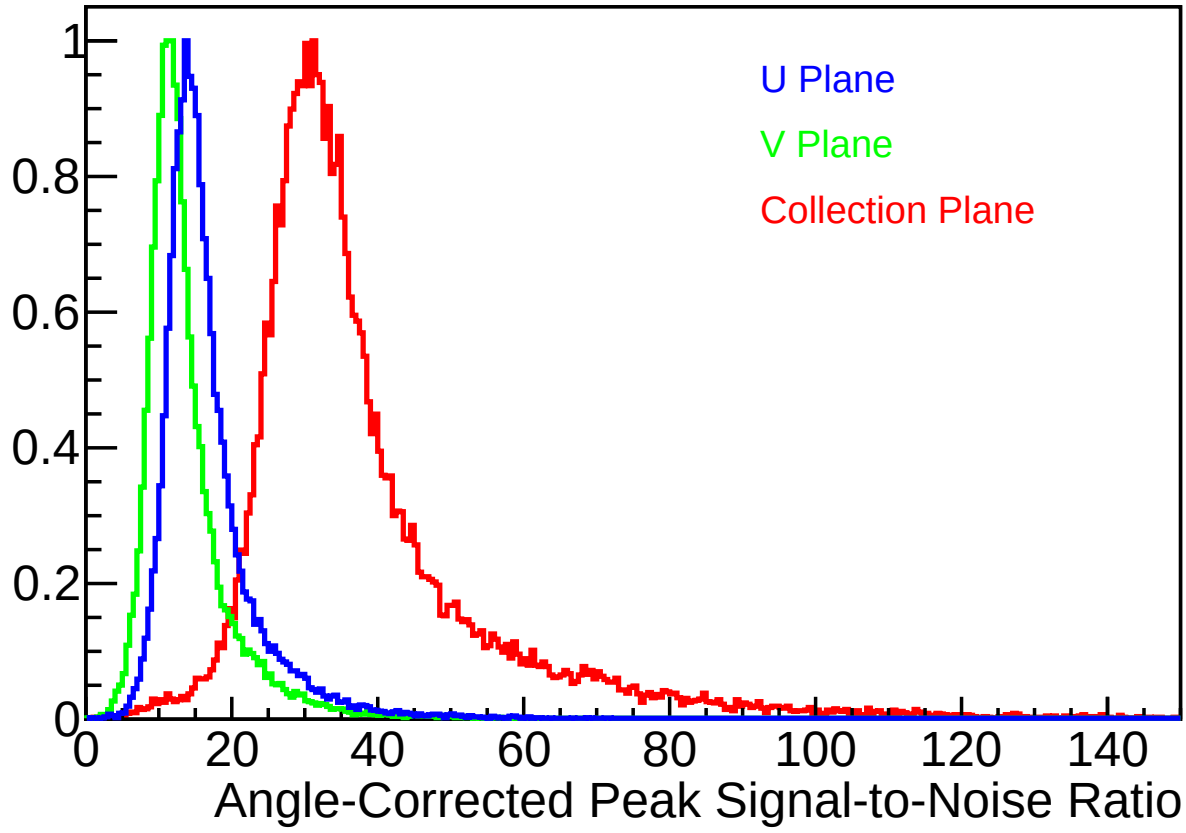

Figure 2: Signal to noise ratio for 3 planes using cosmic ray muons. Author: Heng-Ye Liao.

The signal-to-noise ratio, or SNR, is calculated hit-by-hit. The SNR study has been performed using a sub-run of the run 5432. The signal of each hit is estimated using the maximum pulse height of the raw waveform. The noise value is extracted from a fitted Gaussian sigma on the pedestal distribution of each wire. The SNR has been corrected the signal loss due to the relative angle between a given track and a sensing wire. To minimize the angular dependence of SNR, tracks which are perpendicular to the wire planes are selected. The angle cuts applied on each wire plane are listed as following. The measured SNRs are 30.8, 11.4, and 14.0 for the collection plane, the U plane, and the V plane, respectively.

- **Collection plane**
  - $|\theta_{XZ}| \leq 10°$ and $|\theta_{YZ}| \leq 10°$
  - $170° \leq |\theta_{XZ}| \leq 190°$ and $170° \leq |\theta_{YZ}| \leq 190°$
- **U Plane**
  - Beam Left: $170° \leq |\theta_{XZ}| \leq 190°$ and $-155° \leq \theta_{YZ} \leq -135°$
  - Beam Right: $|\theta_{XZ}| \leq 10°$ and $-45° \leq \theta_{YZ} \leq -25°$
- **V Plane**
  - Beam Left: $|\theta_{XZ}| \leq 10°$ and $-45° \leq \theta_{YZ} \leq -25°$
  - Beam Right: $170° \leq |\theta_{XZ}| \leq 190°$ and $-155° \leq \theta_{YZ} \leq -135°$

3 Data preparation

Data preparation is the first stage in reconstruction of ADC data from the TPC wires. A dynamic pedestal evaluation is done, i.e. for each event (typically 6000 samples for all 15360 channels), the pedestal is evaluated separately for each channel. The ADC counts for most of the samples in each channel cluster in a peak which is fit with a Gaussian after excluding tails from TPC signals and spikes from sticky codes in the ADC. The mean ADC count of this Gaussian is the pedestal for the channel and event and the sigma (RMS) is the pedestal noise. The distributions for the pedestal and pedestal noise in one typical event are shown in Figures 3 and 4, respectively.

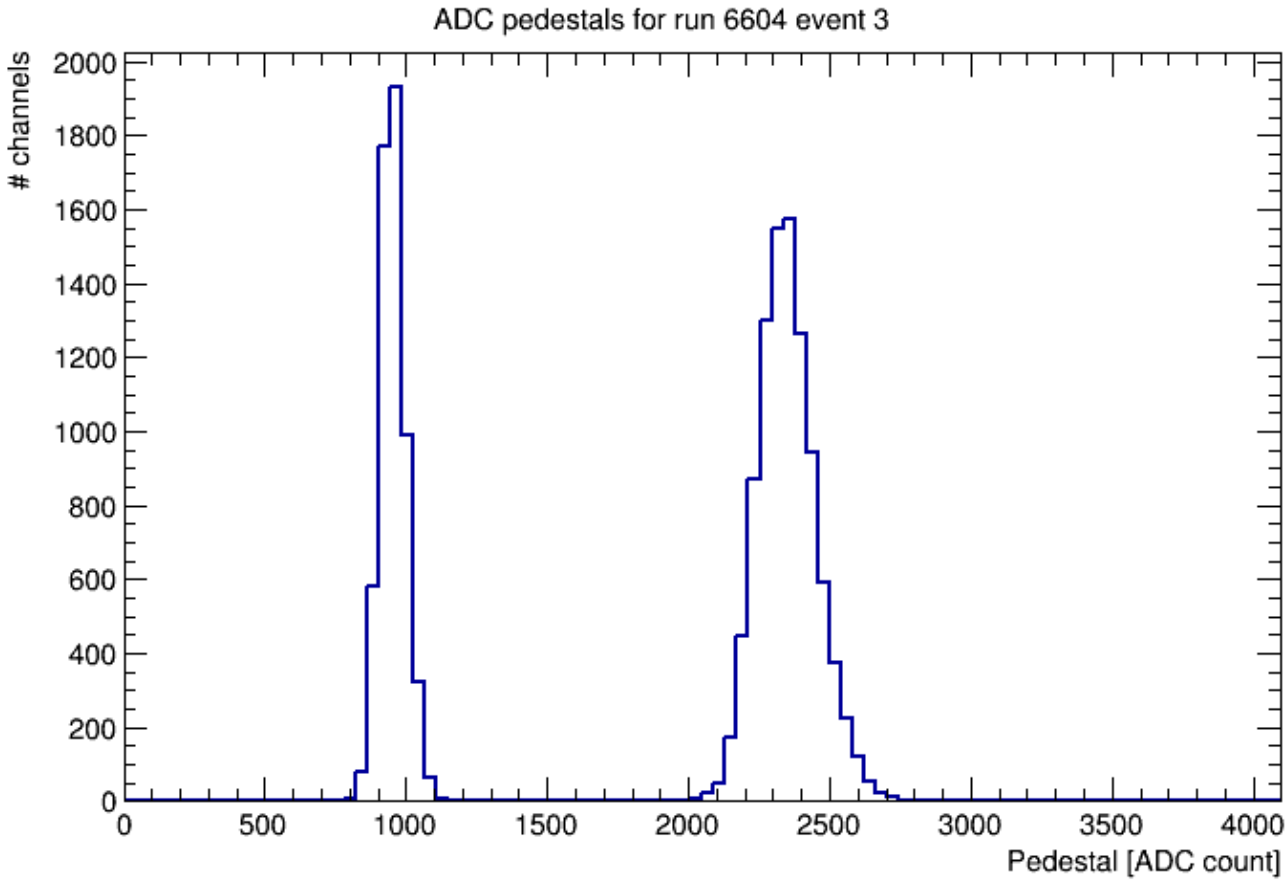

Figure 3: Distribution of pedestals for all TPC channels in one event. The left peak includes the collection channels and the right the induction channels. Author: David Adams

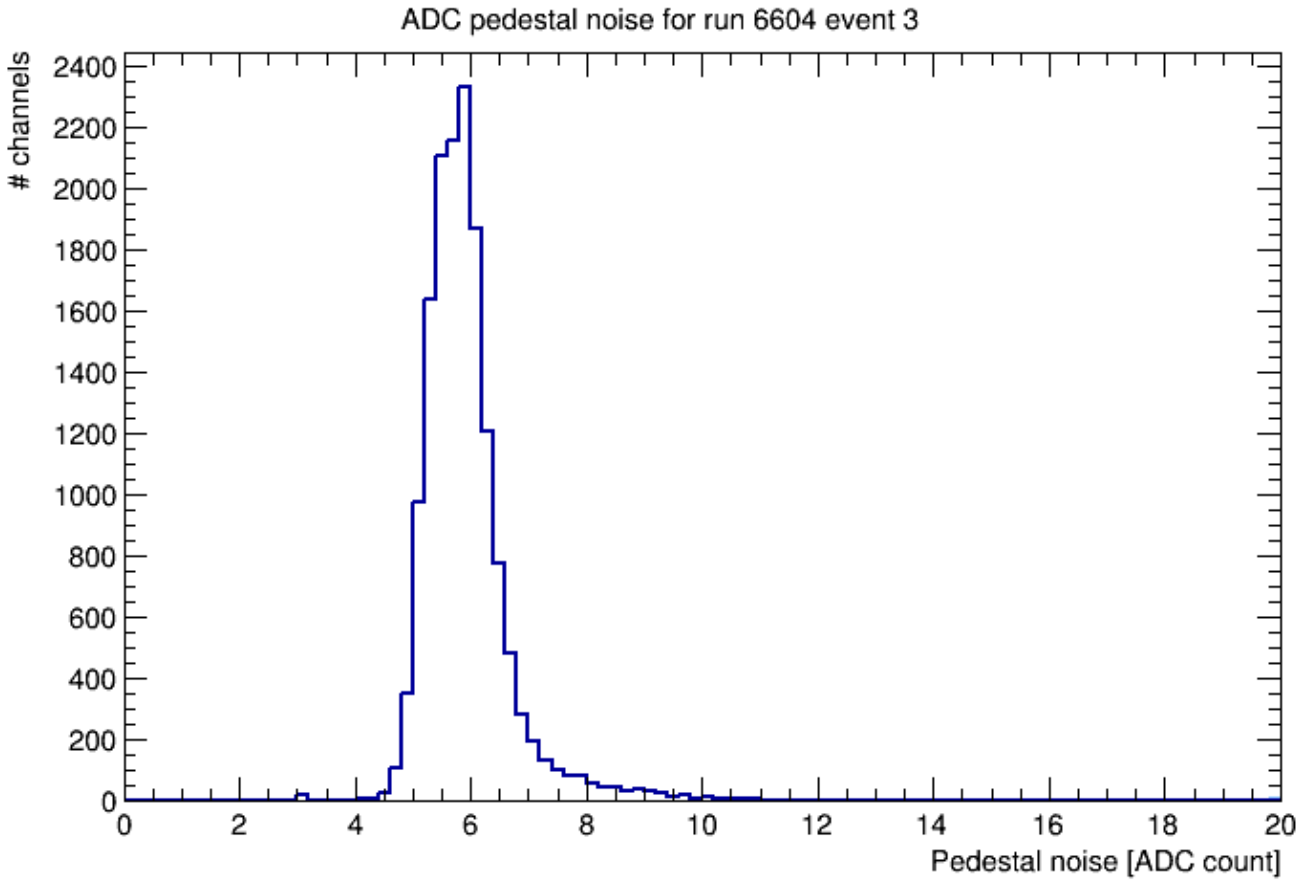

Figure 4: Distribution of pedestal noise for one events. The noise is defined as the sigma of a Gaussian fit of the core of the ADC count distribution for each channel (see text). Author: David Adams

4 Charge calibration

A gain calibration for the TPC electronics (i.e. charge-sensitive amplifier followed by an ADC for each channel) has been carried out using the pulsers in the electronics system. The pulsers rapidly vary the voltage on a capacitor coupled to amplfier input. The voltage alternates between ground and a level that is a programmable integral multiple (*pulser gain*) of approximately 18.75 mV. With the injection capacitance of 183 fF, this corresponds to charge injection of alternating sign with magnitude an integral multiple of 3.43 fC or 21.4 ke. The calibration discussed here used pulser gain settings of 1-7.

The gain is normalized such that summing $Q = gain \times (ADC - pedestal)$ over samples in a pulse gives the charge injected in the amplifier or induced on its wire. In this expression, ADC denotes the ADC count for a sample and the channel's pedestal and gain are indicated. The distribution of gains (i.e. for each channel) is shown in Fig. 5. The mean value is 0.023 ke/(ADC count) and the RMS is 5%. The minimum charge collected for particle traversing the LAr volume associated with a collection wire (i.e. a minimum ionizing particle travelling parallel to the wire plane and perpendicular to the wires) is about 30 ke. With the observed gain, we expect an integrated ADC count of 1300.

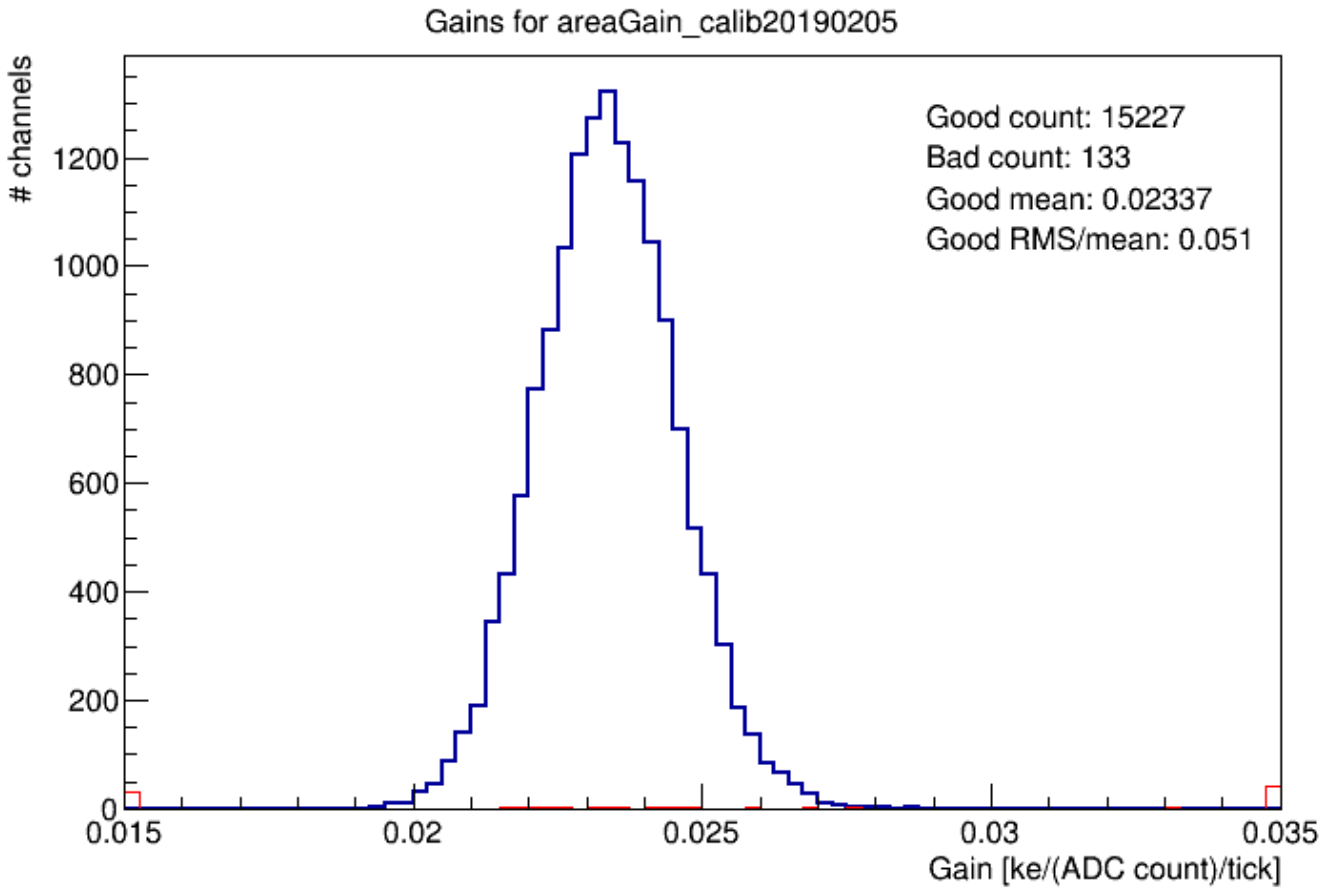

Figure 5: Distribution of ADC gains measured from pulser data (see text). Channels flagged as bad or noisy separately in red. Author: David Adams

5 Charge resolution

Pulser (see Section 4) data is also used to evaluate the local channel charge resolution, i.e. the local uncertainty on the measurement of the charge collected from a track by one wire. This estimate does not include scale uncertainties or response non-linearity. The charge uncertainty is evaluated independently for each channel as the truncated RMS of a distribution of calibrated pulse areas. Figure 6 shows the a typical distribution for all channels. The resolution is about 1.2 ke for collection channels and 1.3 ke for induction channels when the pulse area is integrated over 40 samples. There is a tail of 5-10% of channels with additional noise.

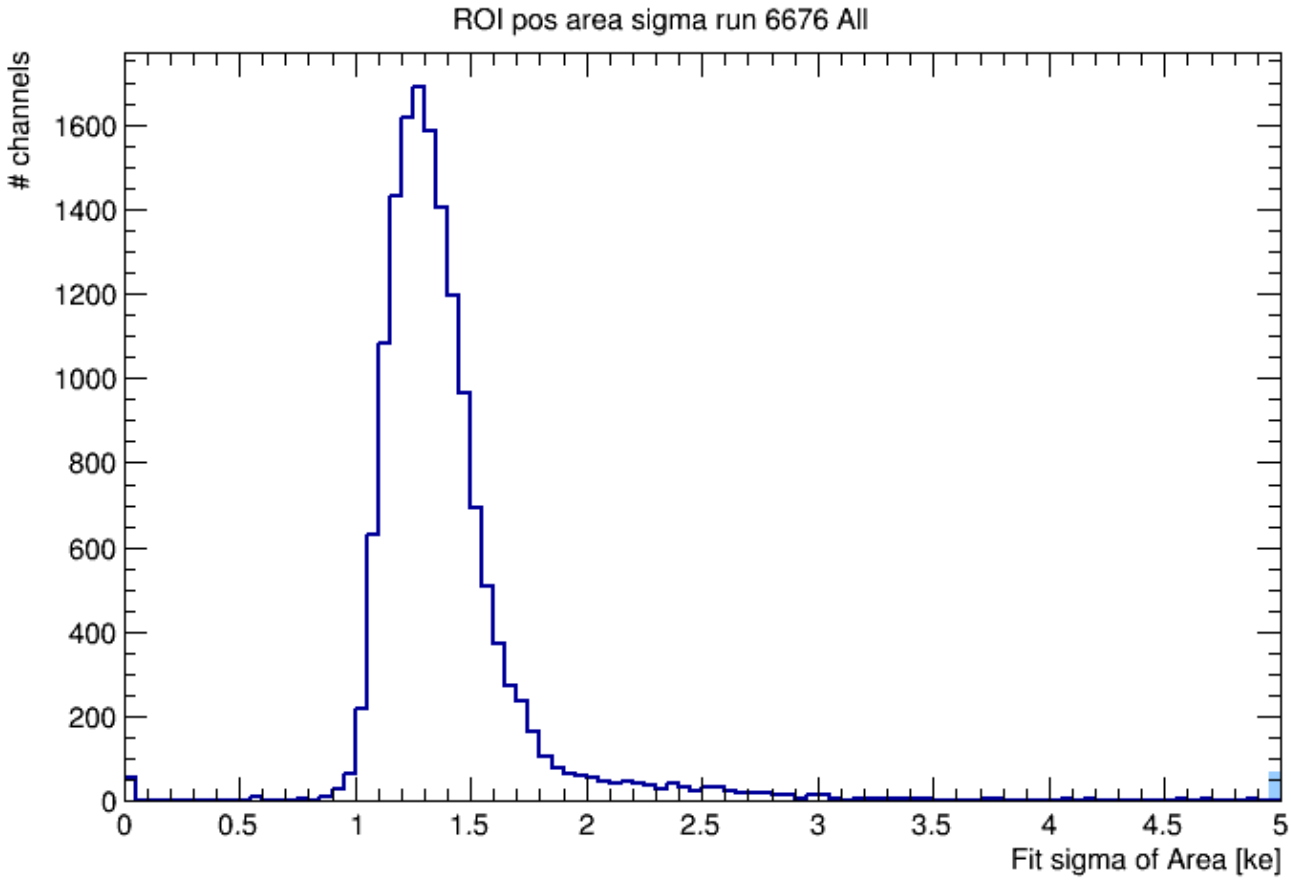

Figure 6: Distribution of local channel resolution with the lowest pulser setting and HV off. Author: David Adams

6 dQ/dx of through-going cosmic ray muons

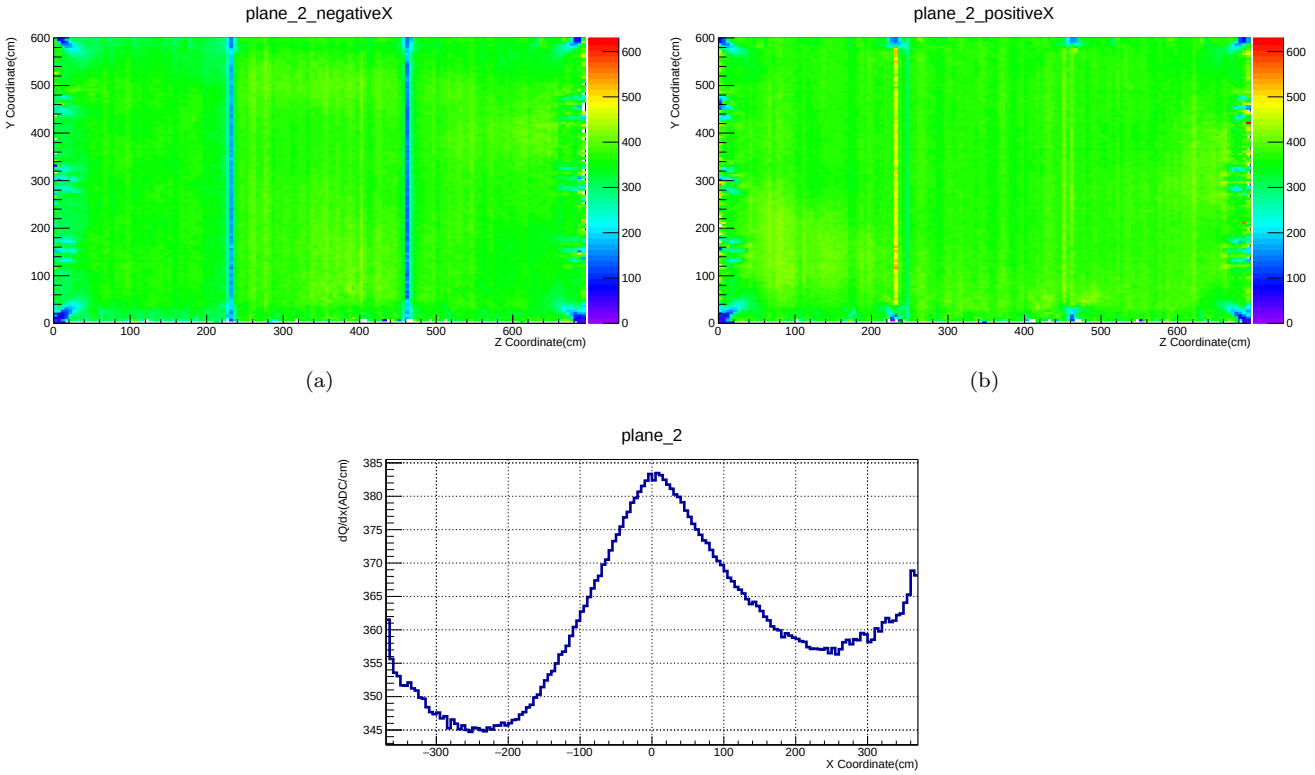

(a) (b)

(c)

Figure 7: dQ/dx distributions as functions of (a),(b) yz and (c) x using cosmic ray cathode crossing muons. Author: Ajib Paudel.

Data sample used: Run 5387, number of events:120430, Tracks are reconstructed using pandoraTrack reconstruction and for Calorimetry information we used pandoracalo.
In plots (a) and (b) for the two drift regions the YZ plane is divided into 5cmX5cm bins and the median dQ/dx value(in ADC/cm) for each such bin is calculated and shown in the plots (c)the whole drift distance is divided into 5cm bins and the median dQ/dx value for each bin is shown.
Following selection cuts were applied to the tracks:

- **Fiducial volume cuts:**Selected CPA piercing(used tracks with a t0 associated with them) and TPC crossing cosmic muons, to make sure they have energy deposition in the MIP region. Used tracks with abs(reconstructed start(end) point X)> 330cm or reconstructed start(end) point Y<50cm or reconstructed start(end) point Y>50cm or reconstructed start(end) point Z<50cm or reconstructed start(end) point Z>550cm.
- **Angular cuts:** Tracks which are parallel to the wire plane or moving straight towards them are not reconstructed well in a LArTPC. We define two angles θ_{XZ} (which is the angle made by the projection of a track on the XZ plane with the Z direction) and θ_{YZ} (which is the angle made by the projection of a track on the YZ plane with the Z direction). Then the tracks with $65° <$ abs$(\theta_{XZ})< 115°$ and $70° <$abs$(\theta_{YZ})< 110°$ are removed.

dQ/dx corrections:
dQ/dx (charge deposition per unit track pitch) varies throughout the TPC due to a number of factors including attenuation due to electro-negative impurities such as O_2, H_2O, space charge effect, diffusion, misconfigured or cross connected TPC channels. To make overall dQ/dx uniform throughout the TPC we apply correction factors

depending on the drift position of the hit. The entire drift distance is divided into 5cm bins and the median dQ/dx value for each such bin is calculated and termed as $(dQ/dx)_{local}$ and the median dQ/dx for the entire TPC is calculated and termed as $(dQ/dx)_{global}$, then the correction factor for a hit at drift coordinate x is given by,

$$C(x) = \frac{(dQ/dx)_{global}}{(dQ/dx)_{local}}$$

We then normalize dQ/dx values to the dQ/dx value at the anode,

$$Normalization factor = \frac{(dQ/dx)_{anode}}{(dQ/dx)_{global}}$$

Finally, the corrected dQ/dx value is given by,

$$(dQ/dx)_{corrected}(x) = (dQ/dx)_{reconstructed} * C(x) * Normalization factor$$

Once we have derived the correction factors to make dQ/dx uniform, we select a sample of cosmic stopping muons and carry out the dE/dx calibrations.

7 dE/dx of stopping cosmic ray muons

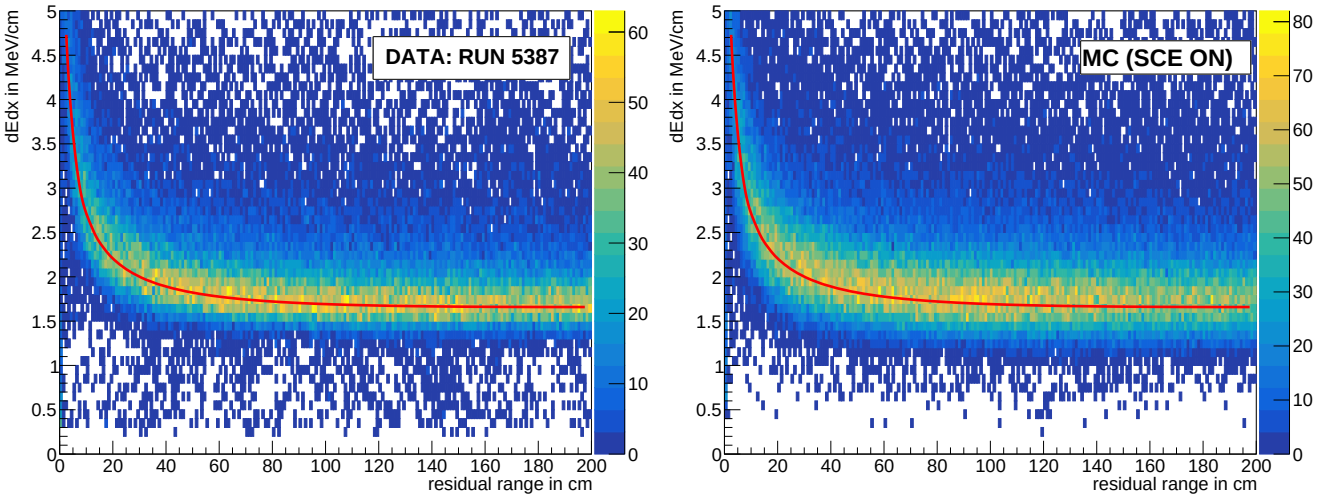

(a) (b)

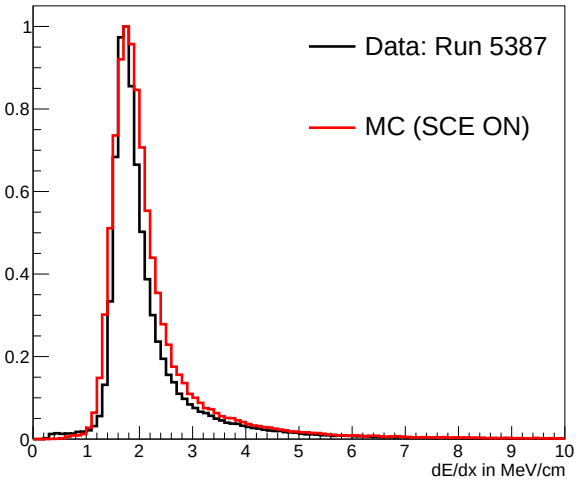

(c)

Figure 8: Stopping muon dE/dx distributions for the ProtoDUNE-SP cosmic data and MC. The red curves in (a) and (b) are the expected most probable value of dE/dx versus residual range. Author: Ajib Paudel.

Data sample used plot(a) Run: 5387, number of events:120430 (b)Space Charge On Monte Carlo sample, number of events:31050 (c)dE/dx distribution for stopping muons
Following selection cuts were used in the data and MC plots above:

- **Fiducial volume cuts**: Stopping cosmic ray muons are used in these plots. Cathode piercing tracks which starts outside the TPC and ends inside the TPC are used. We require abs(reconstructed start point X)> 330cm or reconstructed start point Y<50cm or reconstructed start point Y>550cm or reconstructed start point Z<50cm or reconstructed start point Z>550cm, and abs(reconstructed end point X)< 330cm or 50cm<reconstructed end point Y<550cm or 50cm<reconstructed end point Z<550cm.

- **Angular cuts:**The tracks with $65^\circ < abs(\theta_{XZ}) < 115^\circ$ and $70^\circ < abs(\theta_{YZ}) < 110^\circ$ are removed.
- **Removing Broken tracks:** Some tracks are reconstructed as two or more different tracks, which gives a wrong stopping point. To remove broken tracks we remove any t0 tagged track which has another track (in the same event) within 30cm from it and making an angle less than 14° with it. Additionally, we removed any track which starts or stops within 5cm of APA boundary.
- **Removing tracks with early and late hits**:We removed tracks which started before the time window begins and also those which tracks which does not exit the TPC before the end of the time window, these tracks gives a false impression of being a stopping track. We removed tracks which has minimum value of Hit::PeakT() for the track less than 250 ticks or maximum value of Hit::PeakT() greater than 5900ticks.
- **Removing tracks with Michel hits attached or end point not included in the track:**For this we identified the wire number and Hit::PeakT of the last hit of the track and counted the number of hits not belonging to the track within ±5 wires and ±50 ticks from the last hit of the track. If the count is more than 0 we removed such tracks.

After applying the above selection cuts we get a highly pure sample of stopping muons. We apply the correction factors to the dQ/dx values as described in the previous section. The most probable dE/dx value as a function of residual range for stopping muon tracks in LAr is accurately predicted by Landau-Vavilov theory. From the recorded and corrected dQ/dx values (in ADC/cm) along the muon track in its mip region (120 to 200 cm from stopping point), the dE/dx (in MeV/cm) values is fitted using the Modified Box Model function with the charge calibration constant ($[ADC/cm] \rightarrow [fC/cm]$) as free parameter in the χ^2 minimization. The energy deposit from the stopping muon sample and comparison with the expectation curve in the Figure show the result of the calibration procedure for the run 5387.

8 $dEdx$ of 1 GeV beam muons

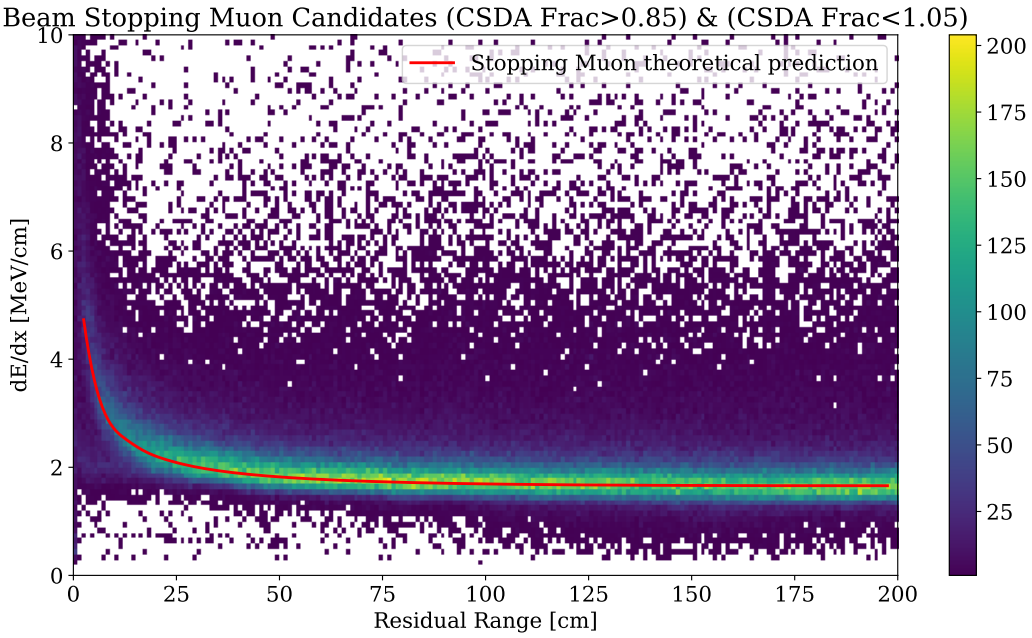

Figure 9: dE/dx vs residual range for stopping muons in the 1 GeV beam after applying the calibration derived using cosmic ray muons. Author: Owen Goodwin.

Stopping muon candidates from the beam were selected from run 5387 (1 GeV beam momentum, HV at 180kV). dE/dx versus residual range for the stopping muon candidates is shown in Figure 9.

The following cuts were used to select these beam stopping muons from data;

- **Beamline Filter**
  The beamline information was used to select events with a time of flight (ToF) $< 170\,\text{ns}$ and no hits in the low pressure Cherenkov counter. This selects primarily pion and muon events.
- **Reconstructed TPC track**
  The Pandora reconstruction algorithm is used to reconstruct and select the beam TPC track candidate.
- **Quality Cuts**
  A series of of quality cuts were placed to select events where the reconstructed track is a true beam particle.
  The cosine angle between the beamline track and the TPC track was required to be greater than 0.93.
- **Position Cuts**
  The following cuts were placed on the difference between the end of the beamline track and the start of the reconstructed TPC track
  - $6.0\,\text{cm} \leq (X^{Start}_{Primary\ track} - X^{End}_{Beam}) \leq 14.0\,\text{cm}$
  - $0\,\text{cm} \leq (Y^{Start}_{Primary\ track} - Y^{End}_{Beam}) \leq 10{,}0\,\text{cm}$
  - $27.0\,\text{cm} \leq (Z^{Start}_{Primary\ track} - Z^{End}_{Beam}) \leq 39.0\,\text{cm}$
- **Stopping Muon Selection**
  The measured beam momentum is used to approximate the range of the particle under the assumption it is

a stopping muon using the continuous-slowing-down approximation range (CSDA range) The variable CSDA Frac is defined as (reconstructed track length/CSDA Range) Tracks with 0.85 <CSDA Frac< 1.05 were selected as beam stopping muon tracks.

Plotted in Figure 9 is the residual range and calibrated dE/dx of the selected tracks. The dQ/dx to dE/dx calibration was performed using values from the cosmic ray muon tracks analysis described above.

9 dE/dx of 1 GeV beam protons

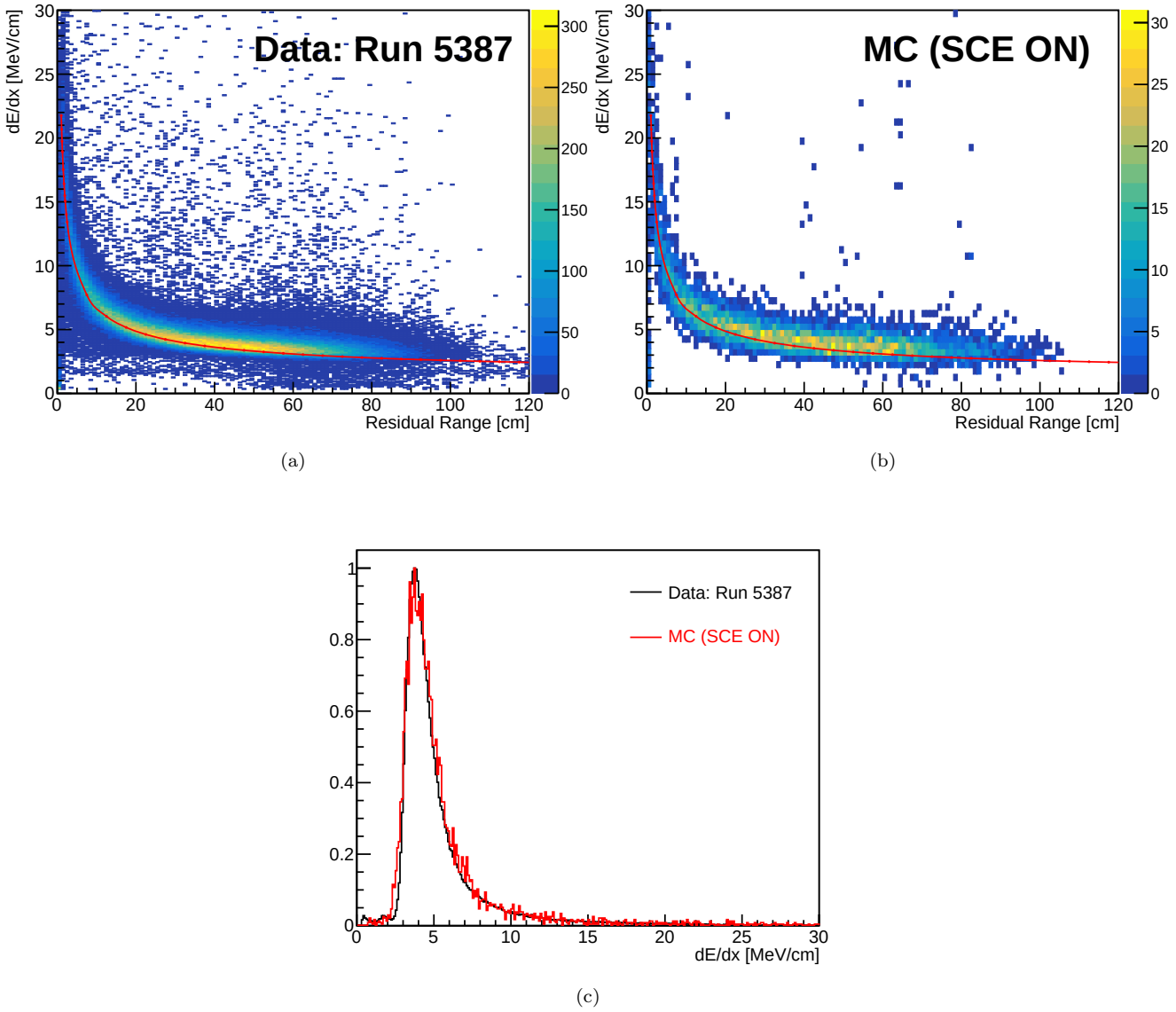

(a) (b)

(c)

Figure 10: Proton dE/dx distributions for the ProtoDUNE-SP 1 GeV beam data (a) and Monte Carlo (b) after applying the calibration derived using cosmic ray muons. The red curves in (a) and (b) are the expected most probable value of dE/dx vs residual range. Figure (c) shows the dE/dx comparison between the data and the Monte Carlo simulation. Author: Heng-Ye Liao.

The run 5387 with 1 GeV/c beam momentum and the applied high voltage at 180 kV was used for the proton analysis. The energy loss as function of a residual range of the stopping protons is shown in Figure 10. The data selection procedure to determine the stopping proton candidates is shown as following.

- **Beamline Filter**
  Particle identification is based on the information from the time-of-flight (ToF) and the Cherenkov counters from the beamline instrumentation. The beam proton events were selected by requiring the value of ToF greater than 170 ns and no triggers from the low and the high pressure Cherenkov counters.

- **Track Reconstruction**
  The Pandora reconstruction algorithm has been used for the beam track reconstruction.

- **Data Cleaning: Angle Cut**
  An angle cut was applied to mitigate the background from other directions. The direction cosine between the beam and the primary proton track was set to be greater than 0.93, with an angle acceptance about 22°.

- **Data Cleaning: Position Cuts**
  The start positions of the primary proton tracks should be close to the positions of the injected beam end-positions. The position cuts were applied and listed as following.
  ◦ $29.8\,\text{cm} \leq (Z^{Start}_{Primary\ track} - Z^{End}_{Beam}) \leq 35.7\,\text{cm}$
  ◦ $0\,\text{cm} \leq (Y^{Start}_{Primary\ track} - Y^{End}_{Beam}) \leq 7.8\,\text{cm}$
  ◦ $6.1\,\text{cm} \leq (X^{Start}_{Primary\ track} - X^{End}_{Beam}) \leq 14.4\,\text{cm}$

- **Stopping Proton Cut**
  The measured beam momentum from the beam instrumentation was translated to its continuous-slowing-down approximation range, or the CSDA range. The stopping proton tracks were selected by comparing the measured track lengths with respect to their expected CSDA ranges. The ratio cut, $0.69 \leq$ (reconstructed track length/CSDA range) ≤ 1.05, was used to select the stopping protons.

After the event selection, the dQ/dx values of the stopping protons were calibrated to their dE/dx values using the cosmic ray muon tracks. The calibration method is described in details in the previous muon dE/dx section. Similar analysis procedure was applied to the Monte Carlo data, with the space charge effect turning on and the simulated electron lifetime of 3 ms. The dE/dx as a function of a residual range of the stopping protons for the data and the MC are shown in Figure 10a and Figure 10b, respectively.

Figure 10c shows the preliminary result of the dE/dx distributions of the data and the MC simulation. The data and the MC are in good agreement. In the MC, the dE/dx resolution is slightly worse than that of the data. This is because we fold in a conservative estimation of the electron lifetime in the simulation.

10 dE/dx of 1 GeV beam positrons

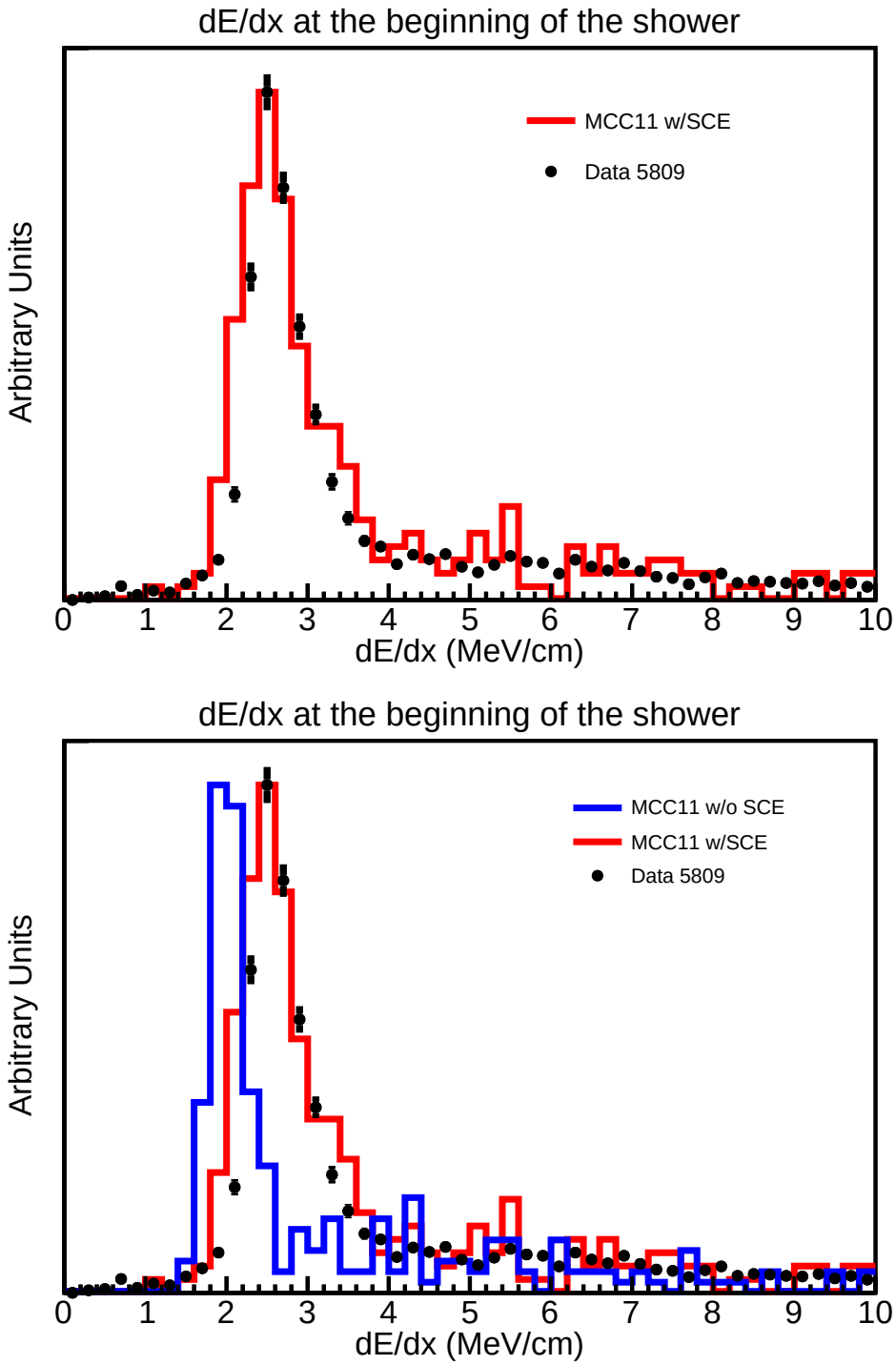

Figure 11: dE/dx distributions of the first 5 cm of the positron events applying the calibration derived using cosmic ray muons. The bottom figure includes two MC distributions. We need to choose which figure to include. Author: Aaron Higuera.

Selection criteria for dE/dx at the beginning of the shower

This analysis uses the official MCC11 w/o SCE and w/SCE and data run 5809. The selection of positron candidates is done as follows:

Data

- Select events with a beam trigger and momentum reconstruction
- Select events with an positron trigger *i.e* $cherenkov[1] == 1$
- Select events where the primary PFParticle is a shower (PandoraShower)
- Select complete shower, where completeness is defined as:

$$completeness = \frac{\text{shower energy}}{\text{beamline momentum}}$$

  See https://indico.fnal.gov/event/19848/contribution/0/material/slides/0.pdf pg, 4.

- Calculate dE/dx at the first 5 cm of the shower

MC

- Select events with a true incoming positron (pdg ==-11)
- Select events where the primary PFParticle is a shower (PandoraShower)
- Select complete shower
- Calculate dE/dx at the first 5 cm of the shower

dE/dx Calculation

Pandora reconstruction does not provide calorimetry so dE/dx is done offline, calculation is done using the association of the shower hits and SpacePoints and shower vertex. dE/dx is calculated for the first 5 cm and only for the collection plane, the median of the dE/dx values for the first 5 cm is used.

11 Photon detector response and resolution

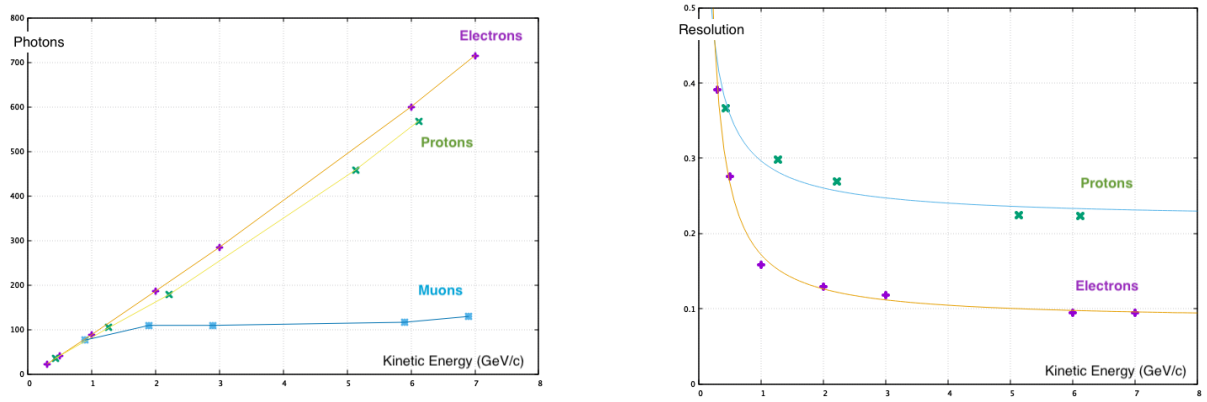

(a) (b)

Figure 12: (a) Photons detected from Arapuca module in APA3 vs kinetic energy.
Particles are classified from beam information: TOF and Cherenkov. For beam momentum 6 and 7 GeV/c, Pandora information is used to distinguish electrons from pions. Muons appear as a second lower peak in the pions spectrum. For electrons and protons the light is proportional to the kinetic energy. Muons reach a plateau after 1 GeV. Since they escape from the cryostat, the energy deposited is the same from 2 GeV to upward.
Subfigure (b) shows the ratio $\frac{\sigma}{<N_{ph}>}$ of the photon distribution for protons and electrons.
The parameterization $\sqrt{a^2 + \left(\frac{b}{\sqrt{x}}\right)^2 + \left(\frac{c}{x}\right)^2}$ was used in the fit [Detectors for Particle Physics. Manfred Krammer. Institute of High Energy Physics, Vienna, Austria]. The "b" parameter which reperest the resolution was found to be: 0.11 ± 0.02 for electrons and 0.20 ± 0.01 for protons.
These very preliminary values should reduce taking into account the spread in the beam momentum.
Author: Dante Totani.

12 Space charge effects

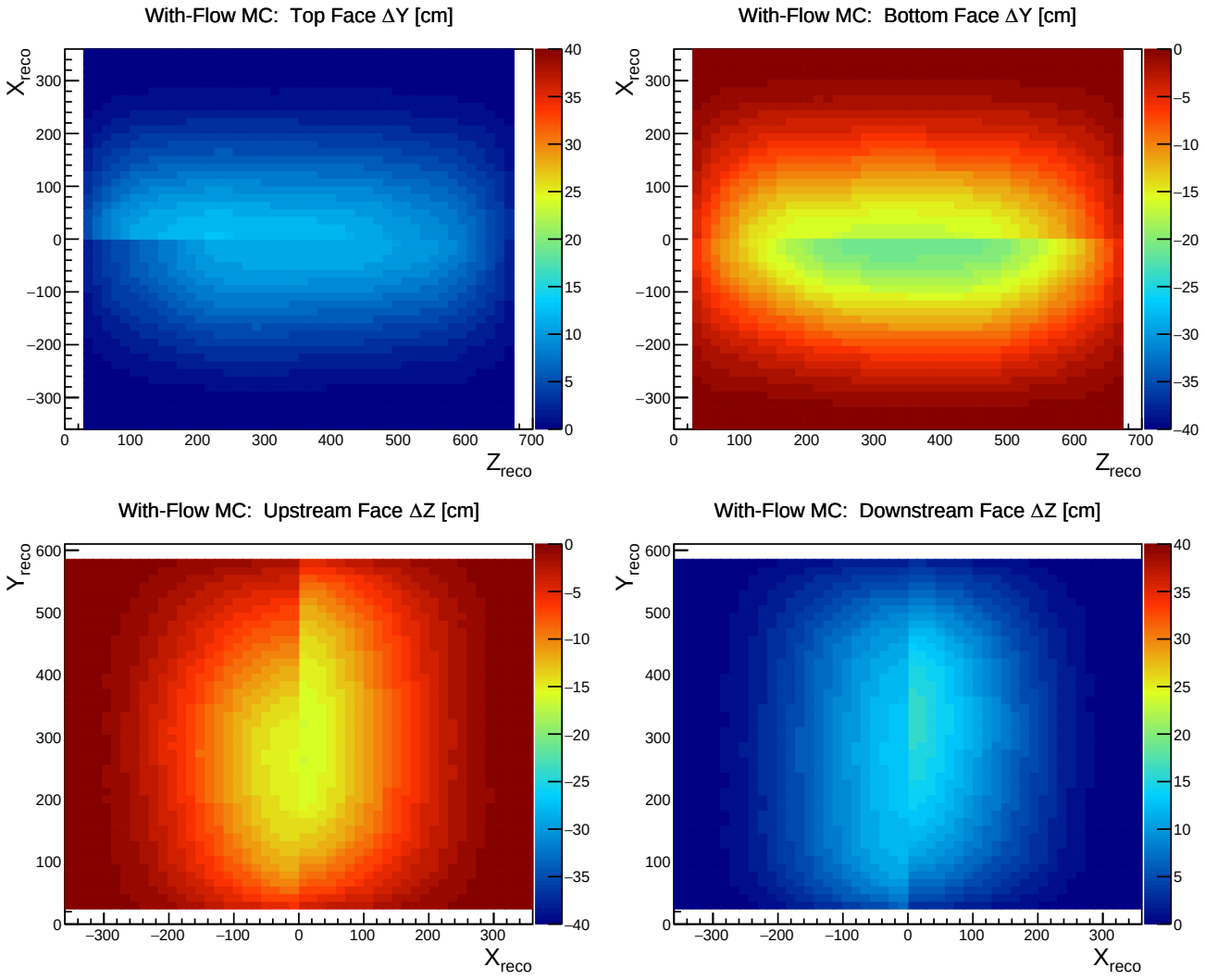

Figure 13: Spatial offsets in MC from various TPC faces in the ProtoDUNE-SP detector due to space charge effects. Shown are offsets from the top (upper left), bottom (upper right), upstream (lower left), and downstream (lower right) TPC faces. Authors: Mike Mooney, Hannah Rogers.

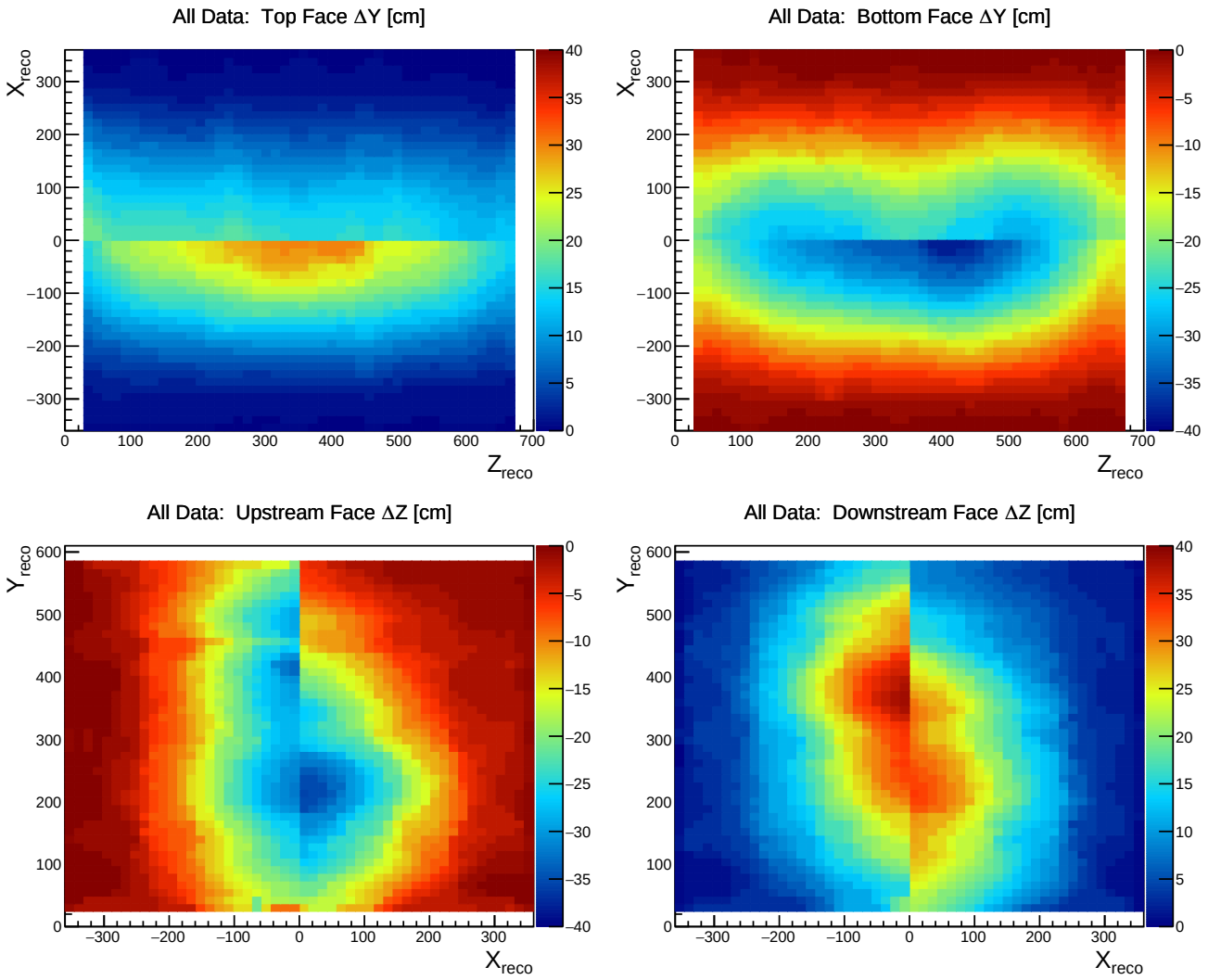

Figure 14: Spatial offsets in data from various TPC faces in the ProtoDUNE-SP detector due to space charge effects. Shown are offsets from the top (upper left), bottom (upper right), upstream (lower left), and downstream (lower right) TPC faces. Authors: Mike Mooney, Hannah Rogers.

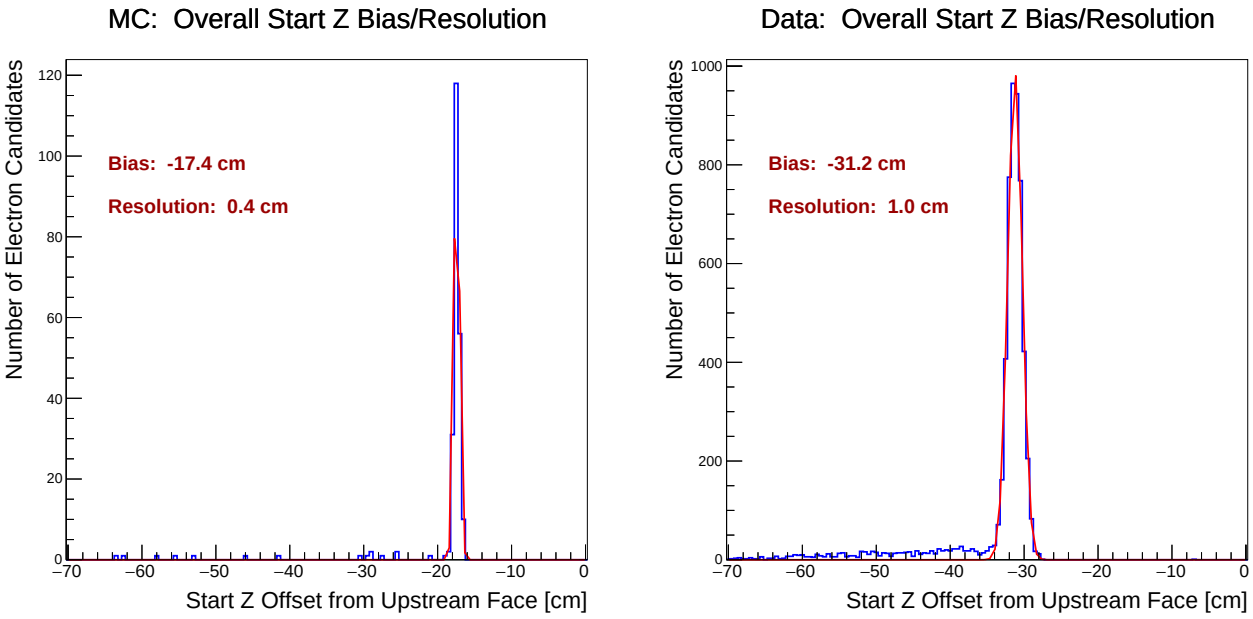

Figure 15: Preliminary study of the time dependence of space charge effects near the region of the detector where charged beam particles enter the active volume. Shown are distributions of the start positions of reconstructed beam electrons in MC (left) and data (right). This study yields an upper limit of roughly 3% on variations of space charge distortions within a single data-taking run (several hours) in this part of the detector. Authors: Mike Mooney, Hannah Rogers, Aaron Higuera.

13 Pandora reconstruction performance

The documentation of these plots is available here `https://docs.dunescience.org/cgi-bin/private/ShowDocument?docid=13214`.

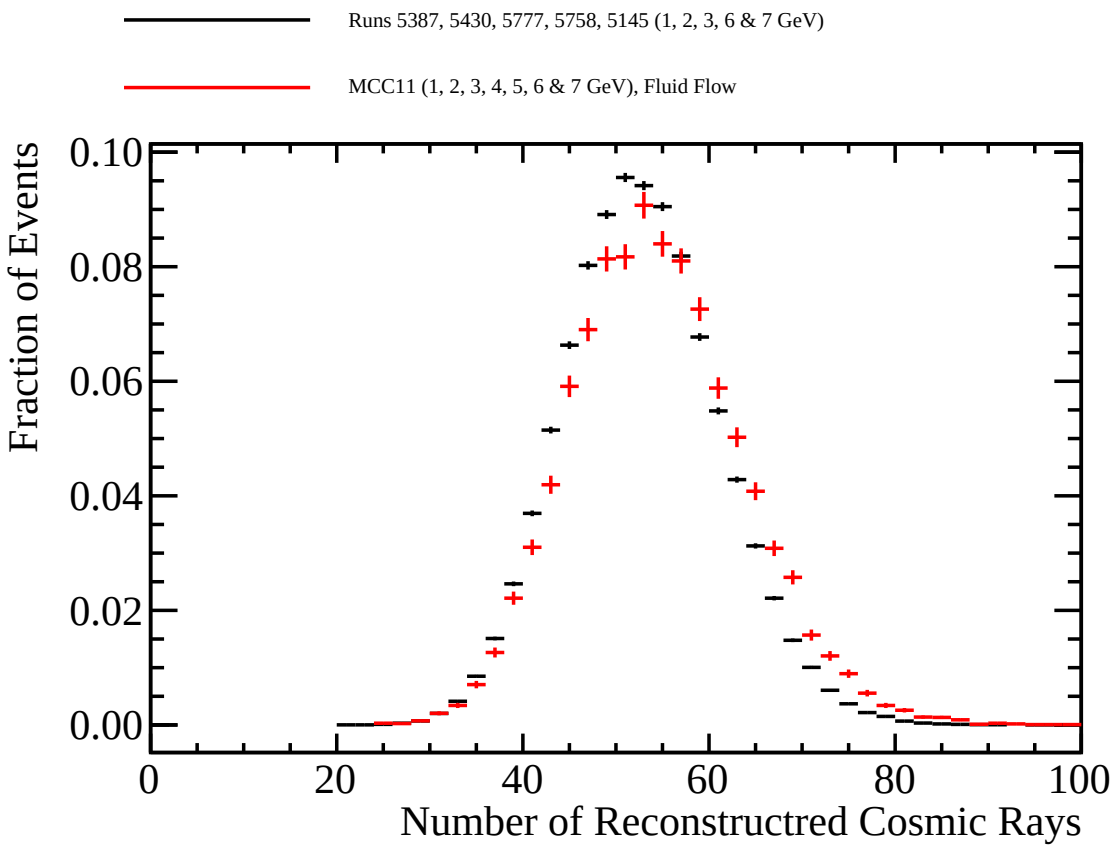

Figure 16: Number of reconstructed cosmic tracks per event in data and MC. Author: Steven Green.

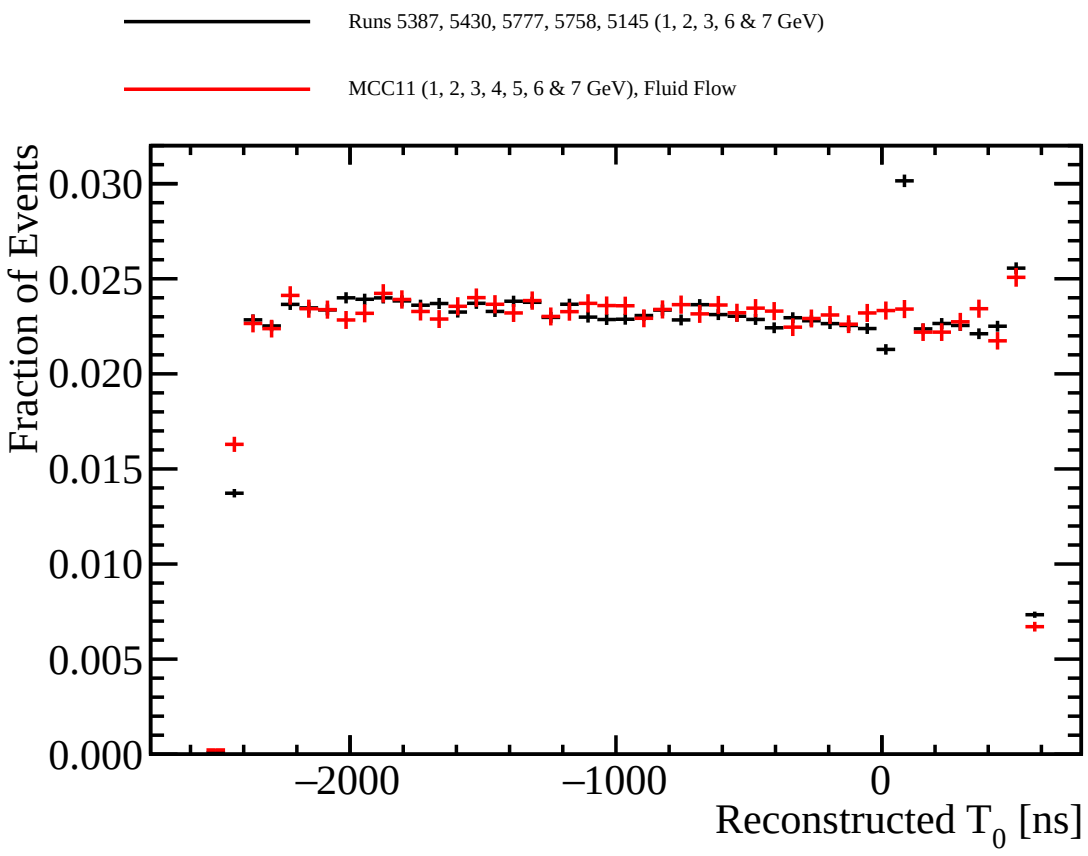

Figure 17: Reconstructed T0 from cathode crossing cosmic tracks. Author: Steven Green.

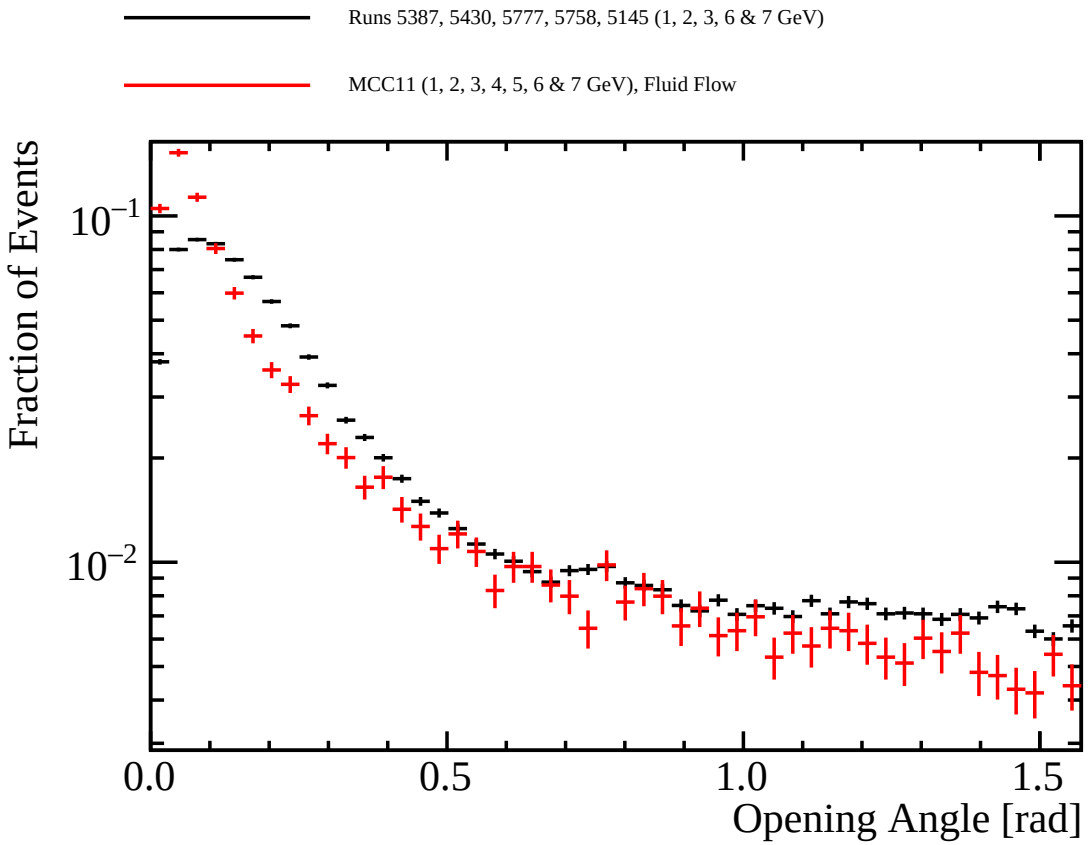

Figure 18: Angular difference between the direction of a reconstructed test beam particle and the expected direction of that particle. Author: Steven Green.

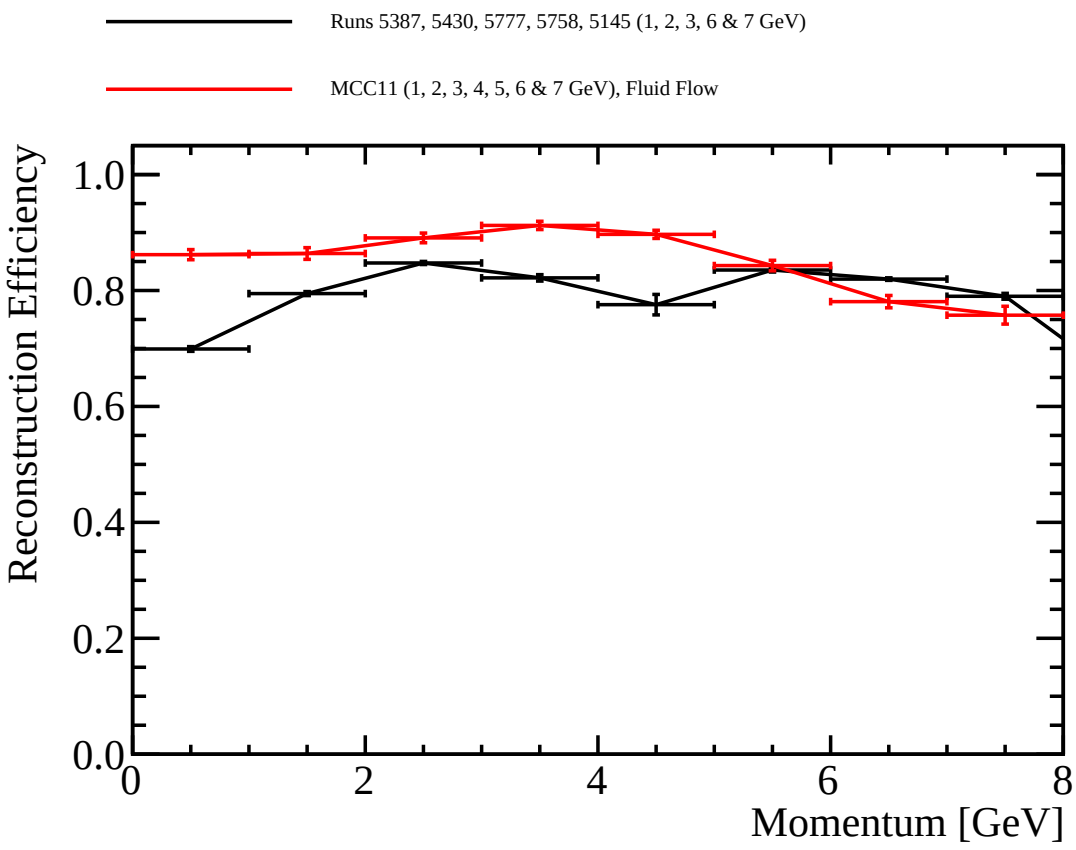

Figure 19: Efficiency to reconstruct a beam particle. Author: Steven Green.

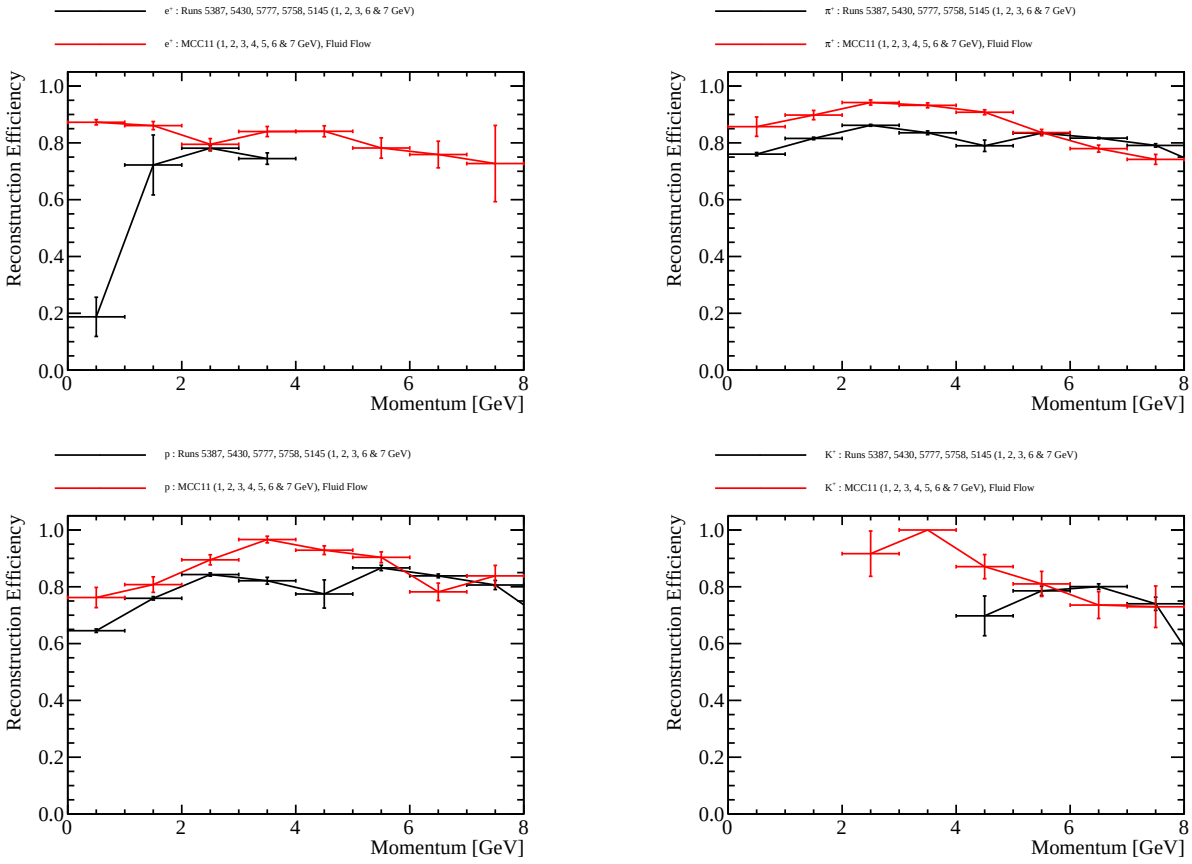

Figure 20: Efficiency to reconstruct a beam particle for different particle species. Author: Steven Green.